



Cy 10

Secondary Gamma Ray Production in Iron and Natural Thorium from Californium Fission Spectrum Neutrons

A. S. Makarious

OAK RIDGE NATIONAL LABORATORY
CENTRAL RESEARCH LIBRARY
DOCUMENT COLLECTION

LIBRARY LOAN COPY

DO NOT TRANSFER TO ANOTHER PERSON

If you wish someone else to see this
document, send in name with document
and the library will arrange a loan.

UCN-7969
(3-67)

OAK RIDGE NATIONAL LABORATORY

OPERATED BY UNION CARBIDE CORPORATION FOR THE ENERGY RESEARCH AND DEVELOPMENT ADMINISTRATION

Printed in the United States of America. Available from
National Technical Information Service
U.S. Department of Commerce
5285 Port Royal Road, Springfield, Virginia 22161
Price: Printed Copy \$4.00; Microfiche \$3.00

This report was prepared as an account of work sponsored by the United States Government. Neither the United States nor the Energy Research and Development Administration/United States Nuclear Regulatory Commission, nor any of their employees, nor any of their contractors, subcontractors, or their employees, makes any warranty, express or implied, or assumes any legal liability or responsibility for the accuracy, completeness or usefulness of any information, apparatus, product or process disclosed, or represents that its use would not infringe privately owned rights.

Contract No. W-7405-eng-26

Neutron Physics Division

SECONDARY GAMMA RAY PRODUCTION IN IRON AND NATURAL THORIUM
FROM CALIFORNIUM FISSION SPECTRUM NEUTRONS

Work performed by:

A. S. Makarious*

Report written by:

A. S. Makarious*

Work directed by:

C. E. Clifford

F. J. Muckenthaler

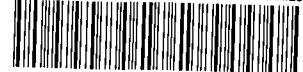
Date Published - March 1977

*On assignment from the Atomic Energy Establishment of Egypt with
Fellowship from the International Atomic Energy Agency

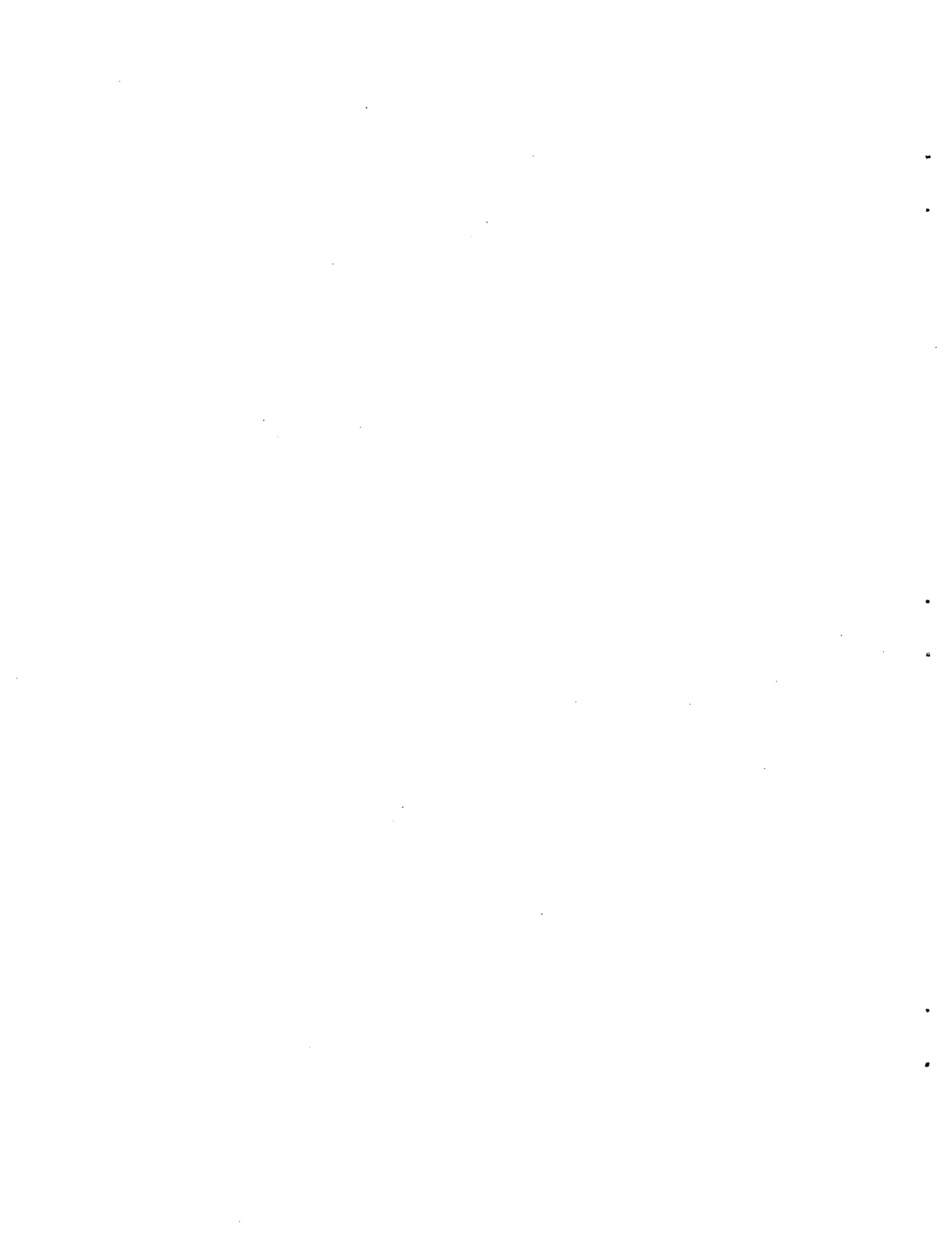
NOTICE This document contains information of a preliminary nature.
It is subject to revision or correction and therefore does not represent a
final report.

OAK RIDGE NATIONAL LABORATORY
Oak Ridge, Tennessee 37830
operated by
UNION CARBIDE CORPORATION
for the
Energy Research and Development Administration

LOCKHEED MARTIN ENERGY RESEARCH LIBRARIES



3 4456 0509714 1



ACKNOWLEDGMENT

A. S. Makarios wants to express his deepest gratitude to Mr. C. E. Clifford and Mr. F. J. Muckenthaler and the TSF Staff for the great efforts and the valuable discussions for the completion of this work. Also I wish to thank E. S. Howe for the preparation of the manuscript.

1950-1951

... ..
... ..
... ..
... ..

... ..
... ..
... ..
... ..

... ..
... ..
... ..
... ..

... ..
... ..
... ..
... ..

... ..
... ..
... ..
... ..

... ..
... ..
... ..
... ..

... ..
... ..
... ..
... ..

TABLE OF CONTENTS

	<u>Page</u>
Abstract.	vii
I. Introduction	1
II. Description of the Experiment.	1
List of Tables.	31
List of Figures	32
References.	33

1. The first part of the document discusses the importance of maintaining accurate records of all transactions and activities. It emphasizes that proper record-keeping is essential for ensuring transparency and accountability in financial reporting.

2. The second part of the document outlines the various methods and techniques used to collect and analyze data. It highlights the need for a systematic approach to data collection and the importance of using reliable sources of information.

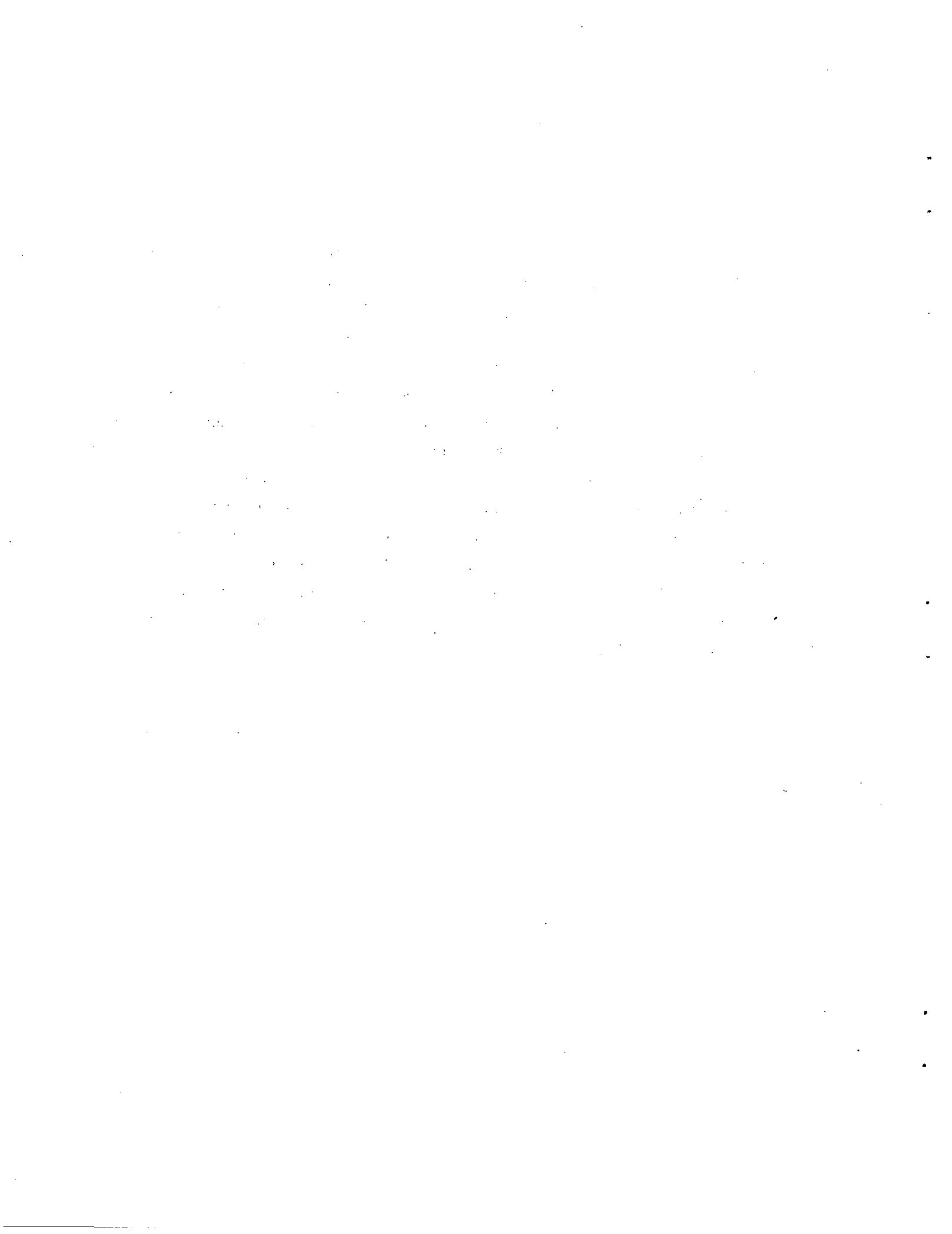
3. The third part of the document focuses on the analysis and interpretation of the collected data. It discusses the various statistical and analytical tools that can be used to identify trends and patterns in the data.

4. The fourth part of the document discusses the importance of communicating the results of the analysis to the relevant stakeholders. It emphasizes the need for clear and concise reporting and the importance of providing context and interpretation of the findings.

5. The fifth part of the document discusses the various challenges and limitations associated with data collection and analysis. It highlights the need for a thorough understanding of the data and the importance of being transparent about any limitations or uncertainties.

ABSTRACT

Measurement of the secondary gamma ray spectra from the interaction of a Cf^{252} fission neutron spectrum with Fe samples of different thicknesses and a Th^{232} sample have been performed at the Tower Shielding Facility at ORNL. A 5-in. by 5-in.-diam NaI (Tl) scintillation spectrometer was used. The measured or .846 MeV gamma ray from neutron inelastic scattering in Fe was compared with calculations using the differential values of cross sections as a function of incident neutron energy. This is an integral check for those differential cross sections. Thorium, as far as we know, had not been investigated before for this fast neutron energy range. Even though a peak at .184 MeV was found it was felt that the resulting large cross section value obtained made it highly improbable that the gamma ray came from a fast neutron interaction. Search for other possible neutron induced gamma rays was very difficult due to the high intensity of naturally radioactive gamma rays from thorium itself.



I. INTRODUCTION

An accurate determination of the secondary gamma-ray production cross sections for shielding materials is a necessary prerequisite for the design and analysis of reactor shields. The primary purpose of the experiments described in this report was to provide an experimental check on the accuracy of these gamma-ray production cross sections. This effort also represents the first phase of a study to evaluate the feasibility for routine evaluations of cross section quantities utilizing a californium source. A sample of iron (different thicknesses) and a sample of thorium were exposed to fission neutrons from the californium source and a measurement was obtained of the resulting gamma-ray spectrum emitted from the sample. The number of neutrons incident on the sample and the yield of photons from the sample were determined absolutely; and since the fission neutron energy distribution is well known, these results can be utilized to get an integral check on the accuracy of the fast neutron cross sections for gamma-ray production.

II. DESCRIPTION OF EXPERIMENTS

A 123 microcurie californium source having an intensity of 2.9×10^8 neutrons per second was utilized in these experiments. The neutrons from the californium source result from spontaneous fission and therefore have a fission neutron distribution. The neutrons were collimated by placing the source in a shield constructed of concrete blocks and paraffin-lithium carbonate bricks. The lithium carbonate bricks lined an opening in the shield ~ 18 cm square and 76 cm deep. The experimental configuration is shown in Fig. 1 and Fig. 2. The distance from the center of the source to the center of the sample was 117.9 cm and the distance from the center of the sample to the top of the source collimator was 40 cm. The source strength at the sample position was determined using a calibrated 4-in.-diam Bonner ball neutron detector. The count rate from the source was determined for a 7.62 cm by 10.16 cm grid of points over the sample surface. A contour map of the neutron intensities obtained from the mapping runs is shown in Fig. 3 and Fig. 4.

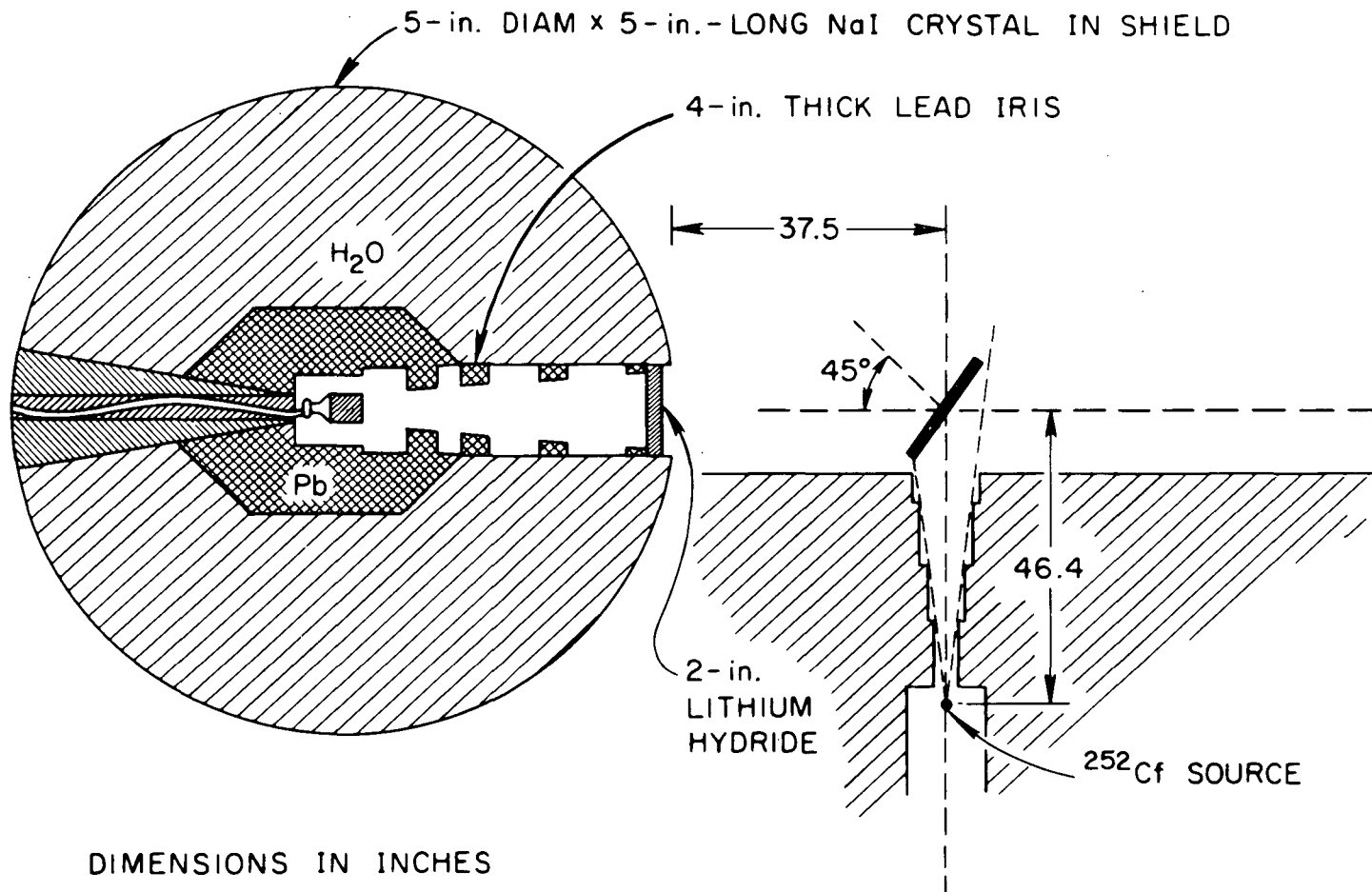


Fig. 1. Schematic Diagram of the Experimental Layout

ORNL-DWG 76-15338

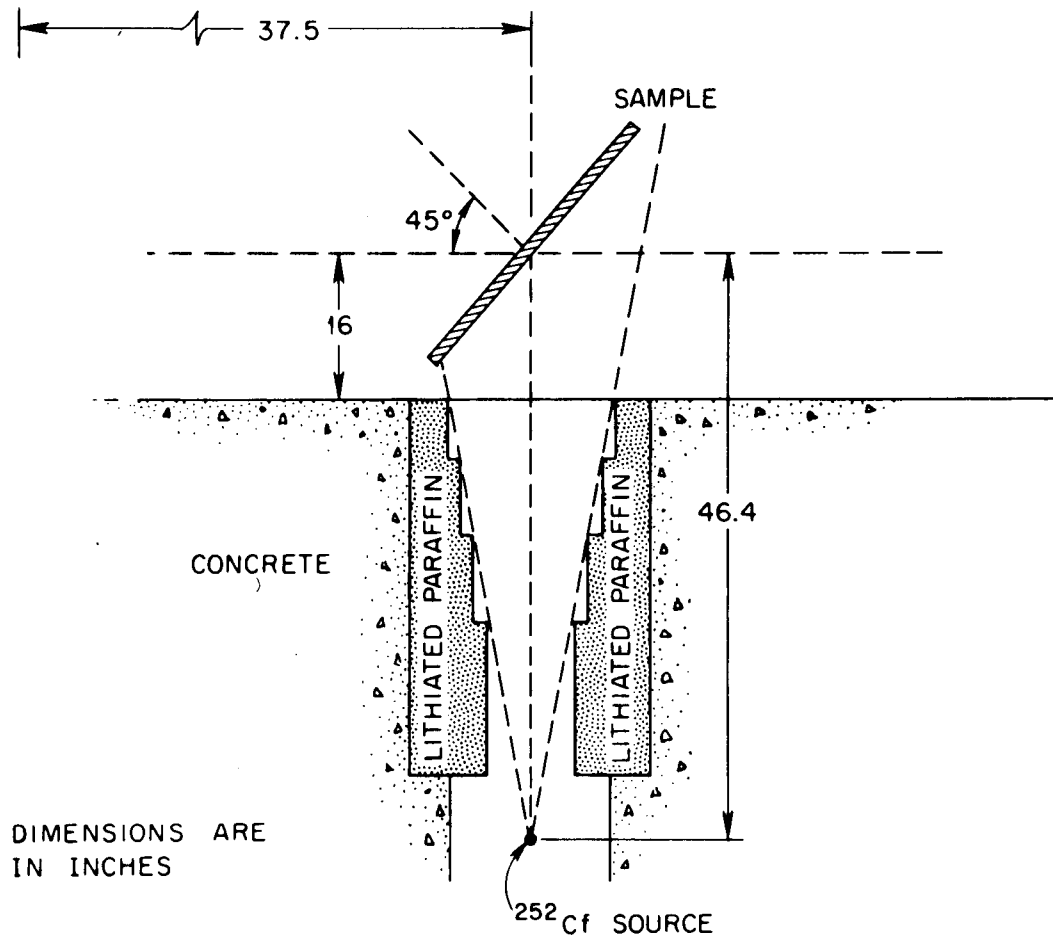


Fig. 2. Schematic Diagram of the Experimental Layout

ORNL-DWG 76-15343

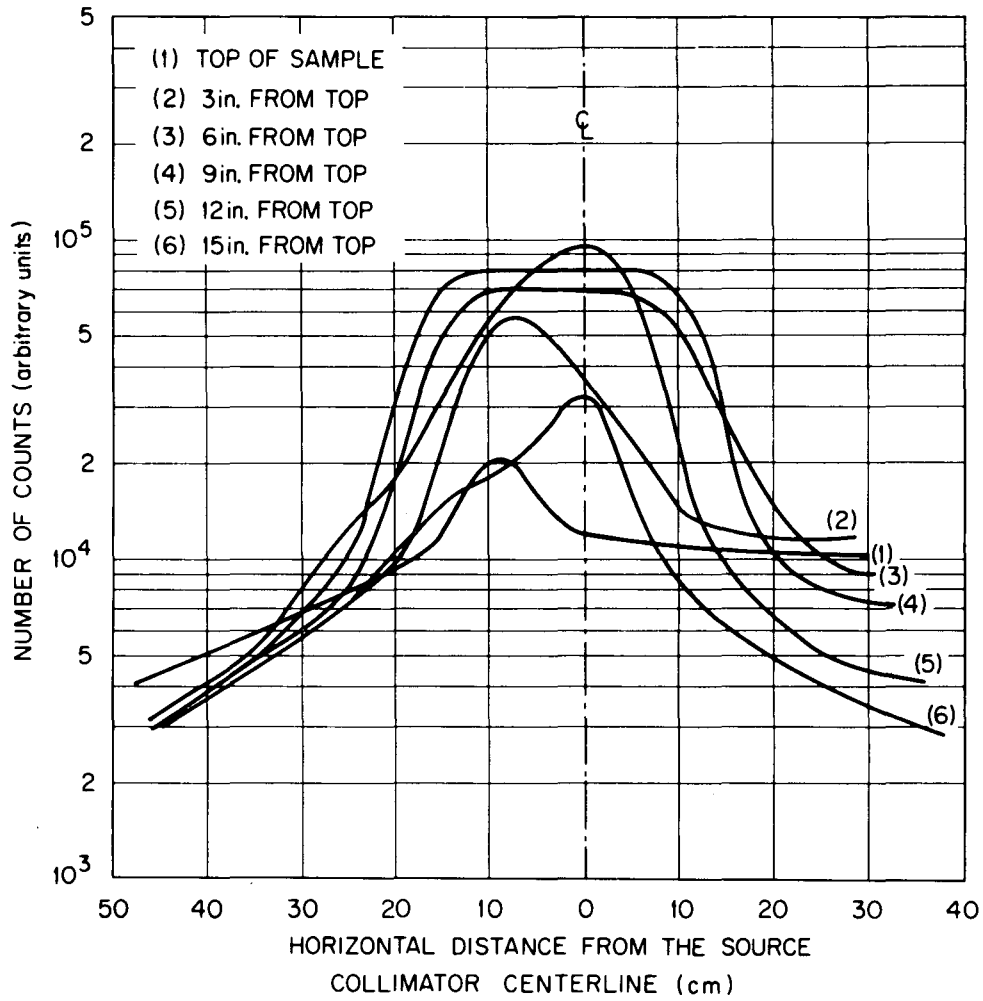


Fig. 3. 4-in. Bonner Ball Mapping of the Neutron Intensity at the Sample Positions

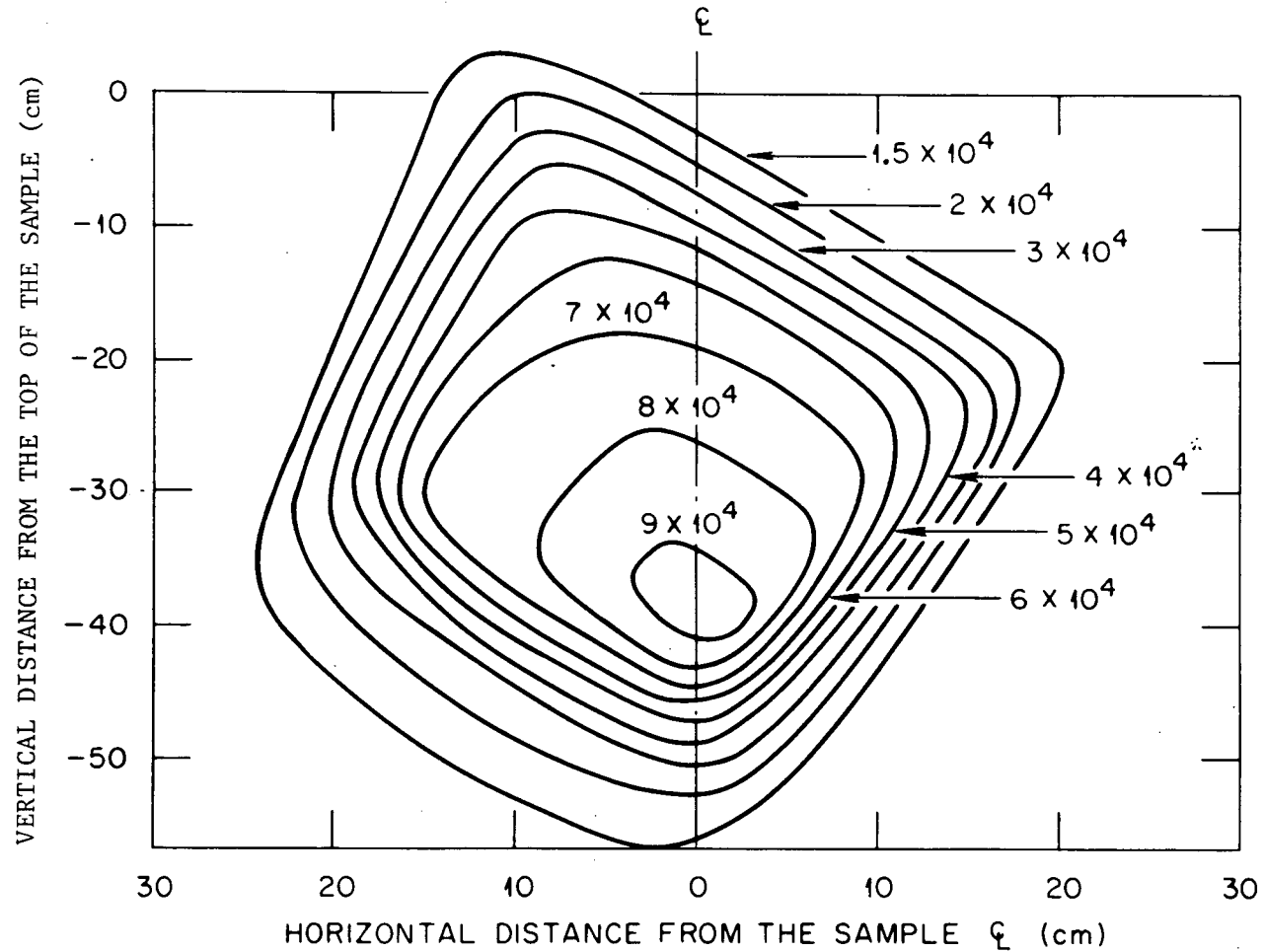


Fig. 4. Isodose Contours of the Fast Neutron Count Rate at the Sample Position Projected in the Vertical Plane (* Arbitrary Units)

Five samples were utilized in this preliminary experimental study. The first four of these were iron slabs \sim .635, 1.27, 1.905, and 2.54 cm thick and 61 cm on the side. The fifth was a cylindrical thorium slab that was 30 cm in diameter and 1.27 cm thick. The samples were positioned at the point where the source collimator centerline intersected the detector collimator centerline. The slab surface was maintained at an angle of 45° with respect to both the detector and source collimator centerlines as shown in Fig. 1. This geometry was chosen to minimize incidence of primary gamma rays from the californium source on the crystal and to reduce to 0.51 MeV or less the energy of these gamma rays scattered by the sample to the crystal.

The gamma ray detector was a 12.7-cm-diam X 12.7-cm-long sodium iodide (Tl) crystal which was positioned to view the sample through a collimator in a very large lead and water shield with a beam port lined with a series of four (10 cm thick) lead irises spaced over a distance of 130 cm from the crystal. The inside edges of the irises were beveled to provide a conical shaped collimator 12.7 cm in diameter at the crystal surface and 31.2 cm in diameter at the outer edge of the last iris. A 5-cm-thick lithium hydride filter was placed against the iris farthest from the crystal to reduce the effect of thermal neutrons on the NaI (Tl) crystal.

Mapping of the detector collimator was carried out using a cobalt source. Vertical and horizontal mappings were done to insure that the axis of the detector collimator intersected the neutron beam centerline at the midpoint of the slab sample and that the NaI detector solid angle encompassed the sample area. Mapping results are given in Figs. 5 and 6 and Tables 1 and 2.

The experimental determination of the absolute response functions for the detector and comparisons with the results of the Monte Carlo calculations, description of the interpolation scheme used in formulating response functions for source energies other than those found experimentally, and a check on these response functions using a relatively well known complex spectrum are described in Reference 1. It is concluded that the response functions are accurate to $\pm 15\%$ over the important

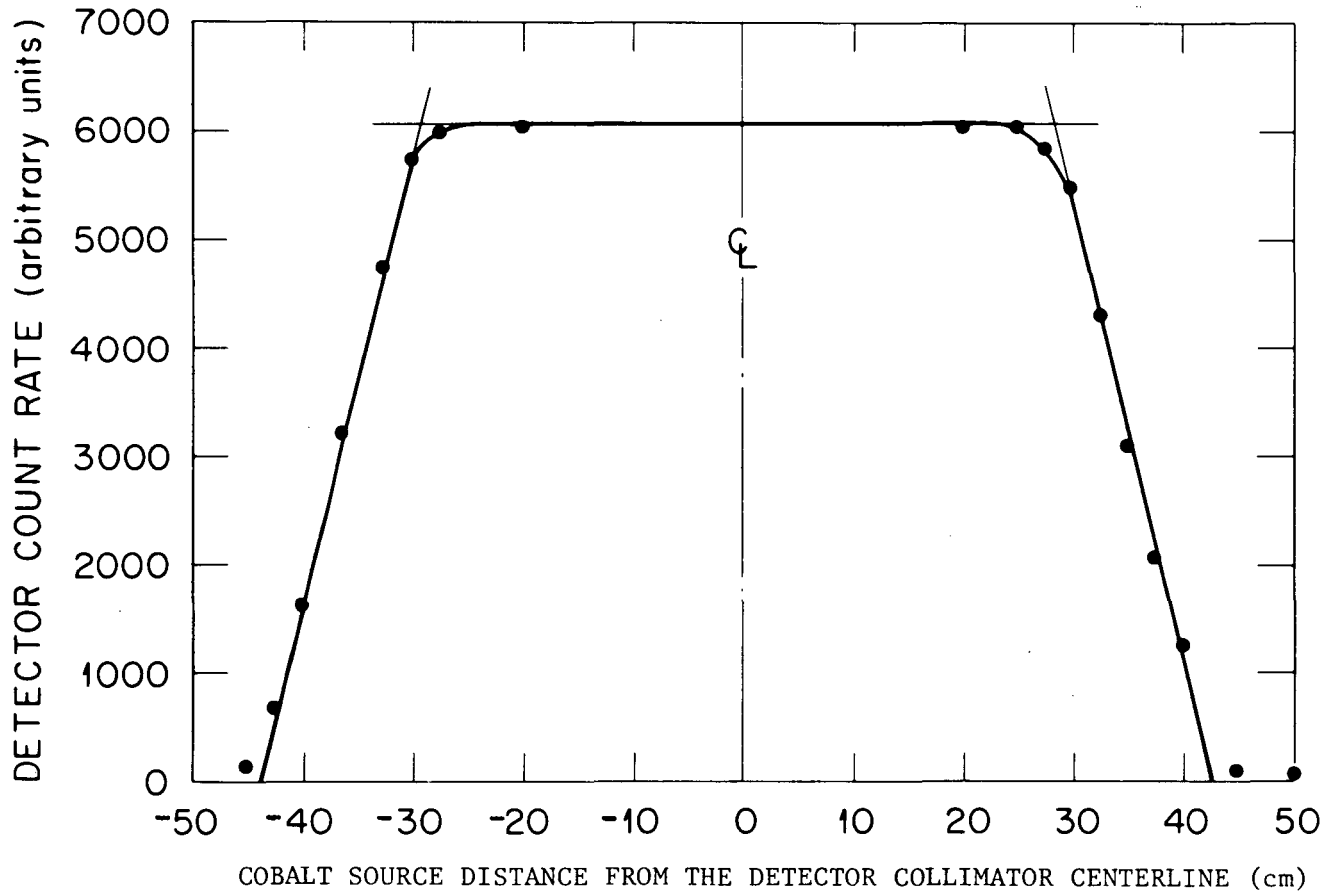


Fig. 5. Vertical Mapping of Detector Collimator with a ^{60}Co Source

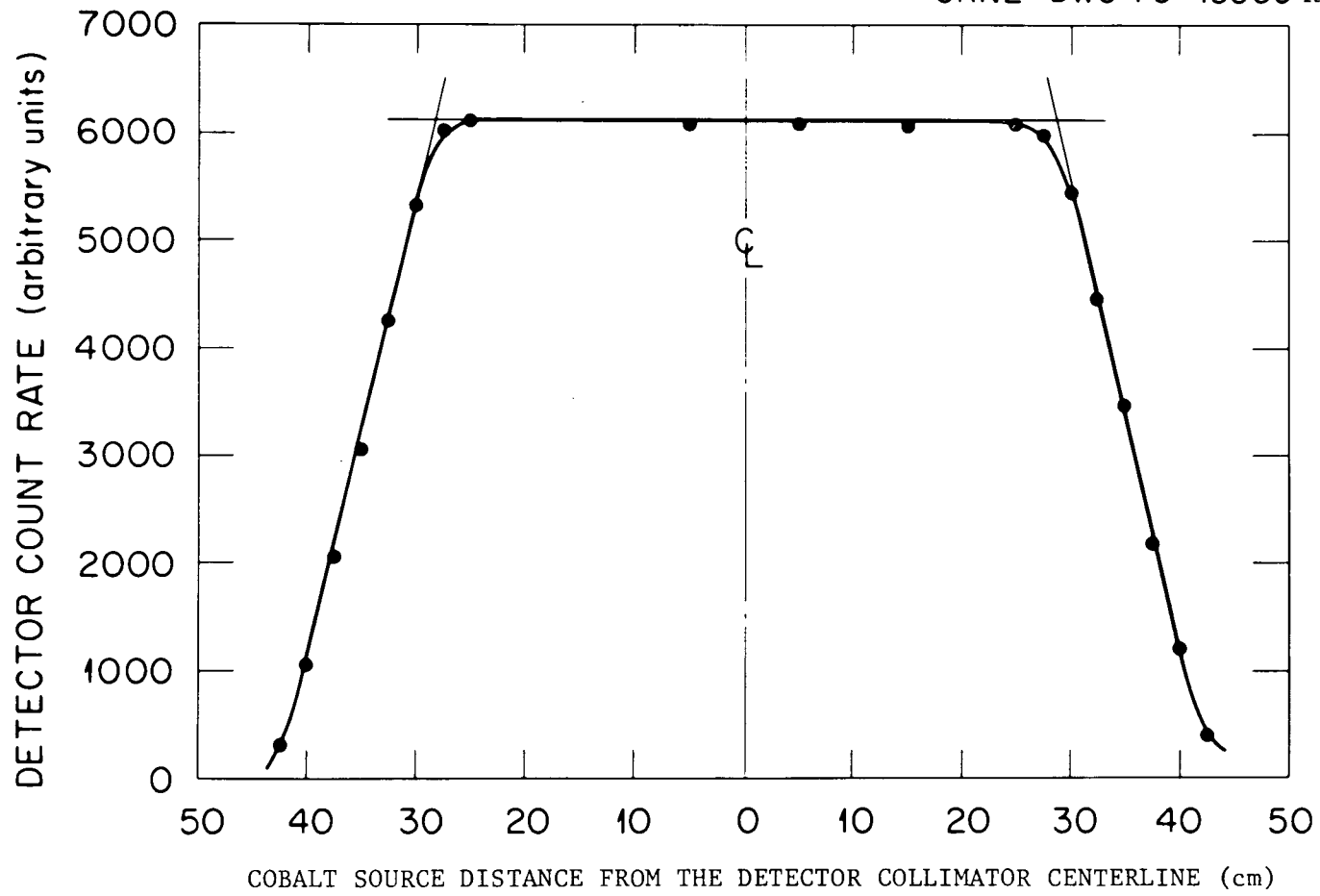


Fig. 6. Horizontal Mapping of Detector Collimator with ^{60}Co Source

Table 1 Vertical Mapping of Detector Collimator

Detector Location From Centerline (cm)	Detector Response (cpm)		
	Run 1	Run 2	Run 3
50	75	84	73
45	99	96	99
40	1254	1204	1194
37.5	2066	2051	2015
35	3107	3183	3066
32.5	4319	4376	4334
30	5453	5392	5356
27.5	5854	5804	5902
25	6068	5976	6018
20	6056	6004	6157
Centerline	—	—	—
-20	6055	6116	6070
-27.5	6006	6021	5965
-30	5743	5637	5731
-32.5	4737	4879	4701
-37.5	3210	3140	3133
-40	1623	1534	1573
-42.5	668	639	600
-45	146	175	170

Table 2 Horizontal Mapping of Detector Collimator

Detector Location From Centerline (cm)	Detector Response (cpm)		
	Run 1	Run 2	Run 2
42.5	303	274	303
40	1048	1015	---
37.5	2056	2004	1980
35	3062	3069	3115
32.5	4245	4290	4265
30	5335	5331	5165
27.5	6018	6051	5881
25	6097	6109	5870
5 S	6072	6124	6178
Centerline	---	---	---
5N	6077	6261	6172
15	6054	6194	6174
25	6074	6093	6033
27.5	5986	5973	6018
30	5431	5564	5622
32.5	4450	4479	4309
35	3449	3556	3547
37.5	2169	2098	2174
40	1180	1093	1185
42.5	359	404	410

pulse height range. The absolute response functions obtained for eight source energies are shown in Fig. 7.

The NaI (Tl) crystal was attached to a RCA 4525 photomultiplier tube that is a matched window type 20MB20/5A-X. Pulses from the photomultiplier tube were fed through a preamplifier (Tennelec Model 021962), a linear amplifier (Tennelec TC-213) into an ADC unit of a transistorized multi-channel pulse height analyzer type ND-2200 (512 channels).

Before each run an energy calibration of the spectrometer was carried out using gamma ray peaks from sources of well known energy, Cr⁵¹ (.320 MeV), Co⁶⁰ (1.17 and 1.33 MeV), neutron capture in H₂O (2.23 MeV), and 4.43 MeV from the C¹² gamma ray in a PuBe source. Since the gamma rays of interest lie below 1 MeV and this energy region would be condensed in a single spectra covering energies up to 12 MeV it was necessary to obtain spectra for two energy bites, one from approximately .2 MeV to 12 MeV and another from approximately .1 MeV to 3 MeV. The high energy spectra is necessary because it affects the values in the low energy region in the unscrambling process. For each sample a foreground measurement and a background measurement for each energy bite were taken. For iron samples the foreground measurements were taken with samples and source in position. The background was taken with the source in position and the sample removed. The difference between the two measurements is due to the effect of the inelastic scattering produced from interaction of fast neutrons from the Cf²⁵² source with the sample. These measurements were repeated several times. The Ferdor Code⁽²⁾ was used for the unscrambling of the spectra (i.e. for transformation from pulse height spectra to energy spectra). The values of the unscrambled spectra are shown in Tables 3, 4, 5, 6 and Figs. 8, 9, 10, and 11. After looking at results for iron slabs of thicknesses ranging from 0.635 cm to 2.54 cm, the 1.27 cm thickness was chosen for the final measurements as the effect of scattering of the secondary gamma rays in the material itself was minimized.

Four runs, one foreground and three backgrounds were necessary to define the inelastically scattered ray peaks in thorium. The thorium sample was contained in a special plastic bag to prevent spread of

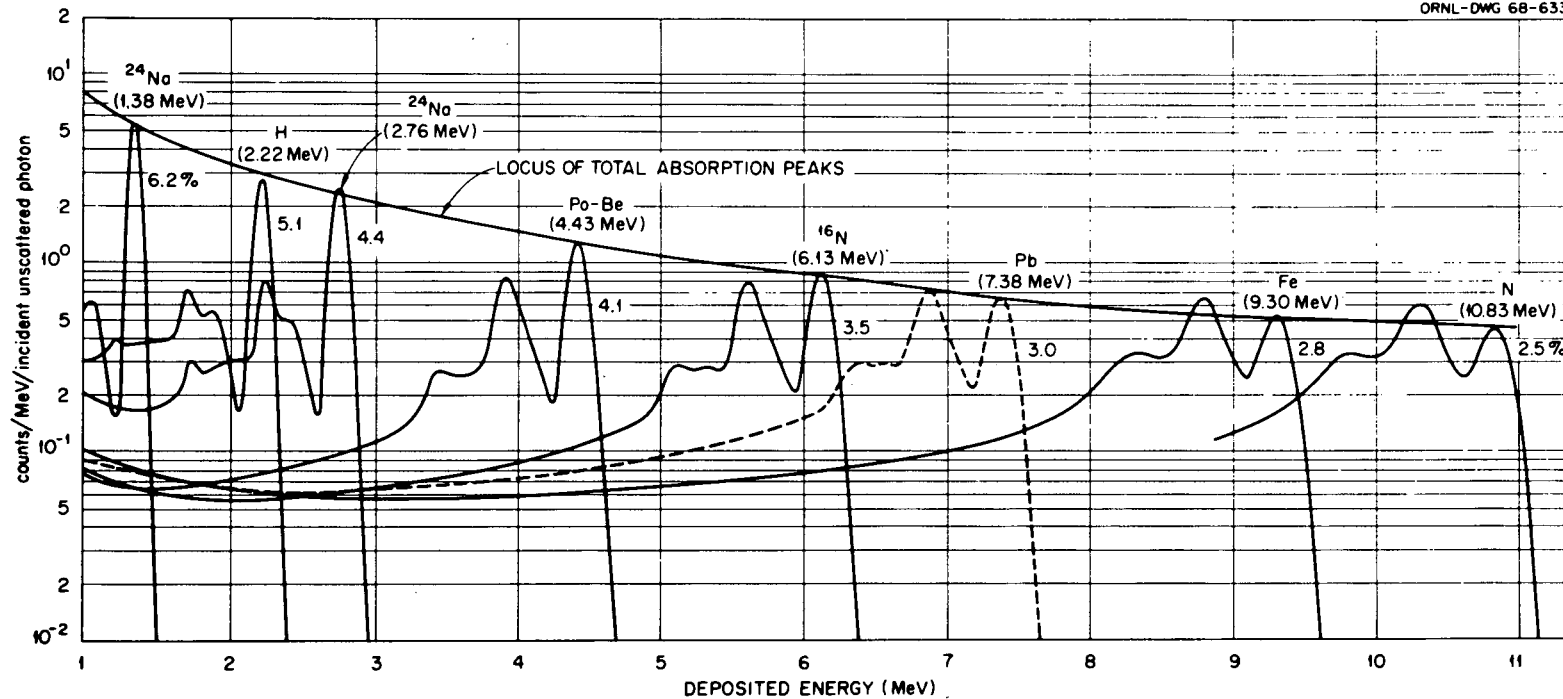


Fig. 7. Absolute Responses for a Shielded and Collimated 5 X 5-in. NaI with 2-in. Borated Polyethylene Neutron Shield Covering the Collimator

Table 3 Gamma Ray Spectral Data for .635 cm Fe

1/4" FE, RUN 846

E1 (MEV)	E2 (MEV)	INTEGRAL (G/S QCM/SEC.)	EFF CR (G/S QCM/SEC.)
0.205	0.300	4.9129E-01	1.6492E-03
0.300	0.400	3.3998E-01	1.4992E-03
0.400	0.500	1.2816E-01	1.0491E-03
0.500	0.600	5.1375E-02	7.4619E-04
0.600	0.700	1.2708E-02	5.7290E-04
0.700	0.800	6.6624E-03	5.4846E-04
0.800	0.900	4.3209E-02	6.2392E-04
0.900	1.000	4.7693E-03	4.5240E-04
1.000	1.100	2.9892E-03	4.0827E-04
1.100	1.200	2.3623E-03	4.6326E-04
1.200	1.300	5.4990E-03	3.8967E-04
1.300	1.400	3.9874E-03	3.8024E-04
1.400	1.500	2.9300E-03	2.4841E-04
1.500	1.600	1.6910E-03	1.9136E-04
1.600	1.800	5.8631E-03	3.5284E-04
1.800	2.000	3.7707E-03	3.0711E-04
2.000	2.200	4.0558E-03	3.1606E-04
2.200	2.400	2.6314E-03	4.3270E-04
2.400	2.600	2.5391E-03	4.1951E-04
2.600	2.800	2.2632E-03	3.9897E-04
2.800	3.000	1.3893E-03	3.8899E-04
3.000	3.500	4.7447E-03	9.4629E-04
3.500	4.000	3.5987E-03	9.5729E-04
4.000	4.500	2.6001E-03	9.4196E-04
4.500	5.000	7.9898E-04	9.0617E-04
5.000	6.000	2.9131E-03	1.7736E-03
6.000	7.000	4.1119E-03	1.5495E-03
7.000	8.000	6.7300E-03	9.7964E-04
8.000	9.000	3.4071E-04	3.8193E-04
9.000	10.000	3.7928E-04	3.3313E-04

Table 4 Gamma Ray Spectral Data for 1.27 cm Fe

1/2 IN. FE + 252CF, RUNS 851A-854A

E1 (MEV)	E2 (MEV)	INTEGRAL (G/SQCM/SEC.)	ERROR (G/SQCM/SEC.)
0.205	0.300	7.8004E-01	1.4919E-03
0.300	0.400	6.2537E-01	1.3888E-03
0.400	0.500	3.0844E-01	1.0233E-03
0.500	0.600	2.1709E-01	7.6628E-04
0.600	0.700	3.8156E-02	4.9114E-04
0.700	0.800	1.9094E-02	4.8057E-04
0.800	0.900	7.9014E-02	5.5182E-04
0.900	1.000	1.9340E-02	3.5961E-04
1.000	1.100	1.5646E-02	3.2380E-04
1.100	1.200	1.0536E-02	3.2231E-04
1.200	1.300	1.4934E-02	2.7570E-04
1.300	1.400	9.9187E-03	2.3290E-04
1.400	1.500	6.1329E-03	1.5919E-04
1.500	1.600	4.0826E-03	1.2863E-04
1.600	1.800	1.0777E-02	2.4200E-04
1.800	2.000	7.3490E-03	2.0444E-04
2.000	2.200	7.9115E-03	2.0185E-04
2.200	2.400	4.0007E-03	1.7530E-04
2.400	2.600	5.4116E-03	1.3440E-04
2.600	2.800	3.4836E-03	1.2330E-04
2.800	3.000	2.7262E-03	1.2213E-04
3.000	3.500	8.8787E-03	3.1318E-04
3.500	4.000	4.4888E-03	3.2692E-04
4.000	4.500	3.5372E-03	3.6726E-04
4.500	5.000	2.5228E-03	3.2596E-04
5.000	6.000	7.3397E-03	5.7581E-04
6.000	7.000	5.0409E-03	4.9108E-04
7.000	8.000	8.6273E-03	3.0608E-04
8.000	9.000	8.9093E-04	2.5455E-04
9.000	10.000	1.7130E-04	2.1709E-04

Table 5 Gamma Ray Spectral Data for 1.905 cm Fe
3/4" FE, RUN 848

E1 (MEV)	E2 (MEV)	INTEGRAL (G/SQCM/SEC.)	ERROR (G/SQCM/SEC.)
0.205	0.300	6.7823E-01	2.6786E-03
0.300	0.400	5.4166E-01	2.5713E-03
0.400	0.500	2.5370E-01	1.8255E-03
0.500	0.600	1.2232E-01	1.2537E-03
0.600	0.700	4.2287E-02	9.2148E-04
0.700	0.800	2.4552E-02	8.8467E-04
0.800	0.900	9.4904E-02	1.0862E-03
0.900	1.000	1.5322E-02	6.5232E-04
1.000	1.100	8.9278E-03	5.7299E-04
1.100	1.200	5.4199E-03	6.1044E-04
1.200	1.300	1.5106E-02	5.5309E-04
1.300	1.400	1.0999E-02	5.0946E-04
1.400	1.500	8.5806E-03	3.6263E-04
1.500	1.600	5.0747E-03	2.9168E-04
1.600	1.800	1.3003E-02	5.4349E-04
1.800	2.000	1.1132E-02	4.7389E-04
2.000	2.200	1.0987E-02	4.6523E-04
2.200	2.400	5.6646E-03	4.0861E-04
2.400	2.600	4.8658E-03	3.6166E-04
2.600	2.800	6.0196E-03	3.4986E-04
2.800	3.000	3.5873E-03	3.4137E-04
3.000	3.500	1.0011E-02	8.3694E-04
3.500	4.000	8.8952E-03	8.6392E-04
4.000	4.500	4.4811E-03	9.0553E-04
4.500	5.000	4.1019E-03	8.4990E-04
5.000	6.000	6.9731E-03	1.5764E-03
6.000	7.000	8.4310E-03	1.3875E-03
7.000	8.000	1.3106E-02	1.0358E-03
8.000	9.000	9.3356E-04	7.8630E-04
9.000	10.000	9.2695E-04	7.4747E-04

Table 6 Gamma Ray Spectral Data for 2.54 cm Fe

1" FE, RUN 849

F1 (MEV)	E2 (MEV)	INTEGRAL (G/SQCM/SEC.)	ERROR (G/SQCM/SEC.)
0.205	0.300	5.6915E-01	2.4748E-03
0.300	0.400	4.8514E-01	2.4395E-03
0.400	0.500	2.5083E-01	1.7938E-03
0.500	0.600	1.2621E-01	1.2465E-03
0.600	0.700	4.9232E-02	9.3777E-04
0.700	0.800	2.9706E-02	9.1153E-04
0.800	0.900	1.0280E-01	1.1014E-03
0.900	1.000	1.7129E-02	6.5161E-04
1.000	1.100	1.0003E-02	5.7029E-04
1.100	1.200	6.6823E-03	6.1148E-04
1.200	1.300	1.6142E-02	5.5552E-04
1.300	1.400	1.2259E-02	5.0324E-04
1.400	1.500	1.0102E-02	3.6526E-04
1.500	1.600	6.5434E-03	2.9930E-04
1.600	1.800	1.4764E-02	5.5284E-04
1.800	2.000	1.3285E-02	4.8941E-04
2.000	2.200	1.1916E-02	4.7474E-04
2.200	2.400	6.8760E-03	4.2205E-04
2.400	2.600	6.6075E-03	3.7459E-04
2.600	2.800	7.0929E-03	3.5957E-04
2.800	3.000	4.1156E-03	3.4993E-04
3.000	3.500	1.1736E-02	8.6394E-04
3.500	4.000	1.0191E-02	8.9374E-04
4.000	4.500	5.4150E-03	9.4806E-04
4.500	5.000	4.9320E-03	8.8118E-04
5.000	6.000	8.7286E-03	1.6189E-03
6.000	7.000	9.6639E-03	1.4111E-03
7.000	8.000	1.4151E-02	1.0297E-03
8.000	9.000	8.0782E-04	7.7665E-04
9.000	10.000	9.1662E-04	6.5977E-04

1/4' FE, RUN 846

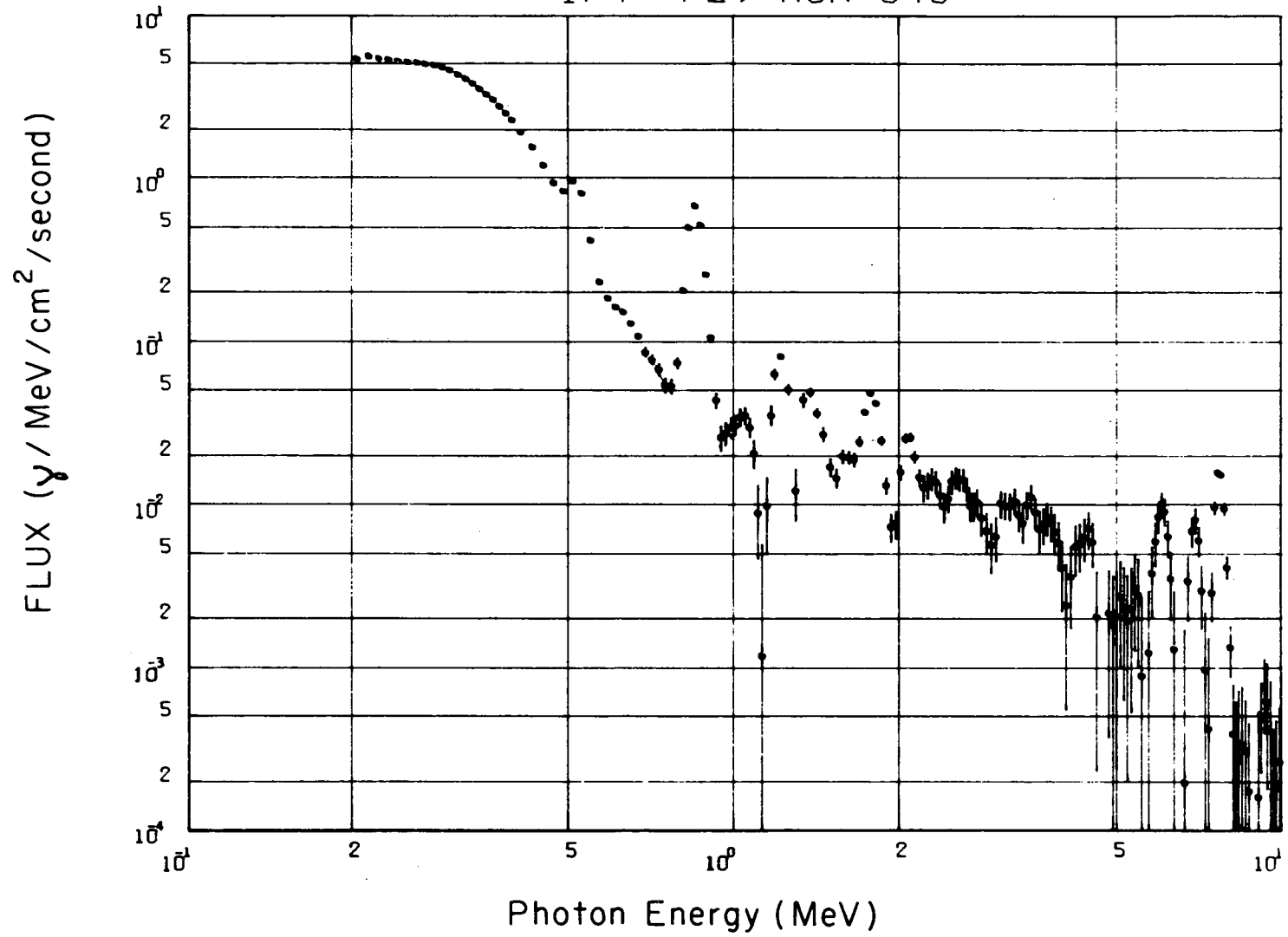


Fig. 8. Gamma Ray Spectra for .635-cm-thick Fe Sample.

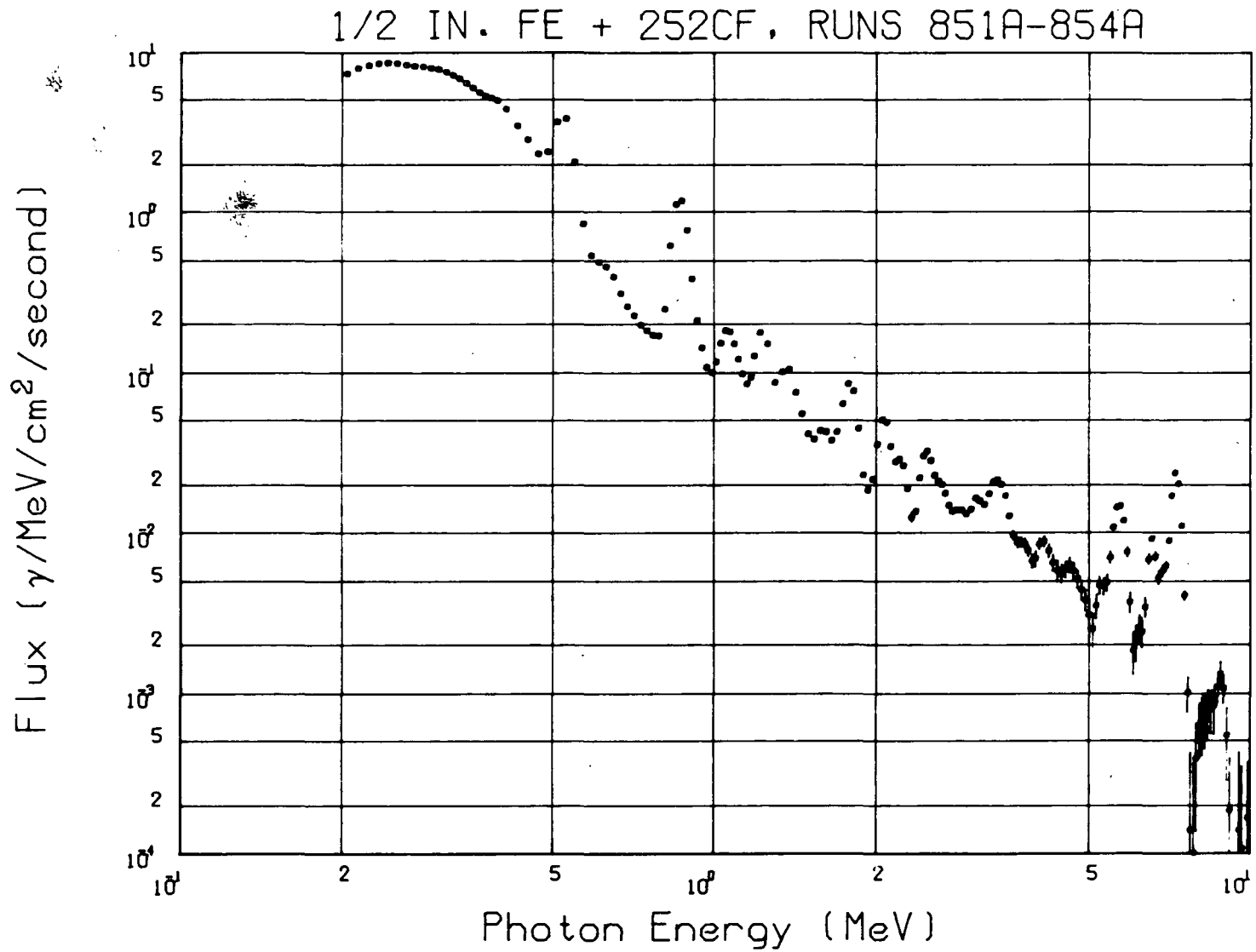


Fig. 9. Gamma Ray Spectra for 1.27-cm-thick Fe Sample

3/4' FE, RUN 848

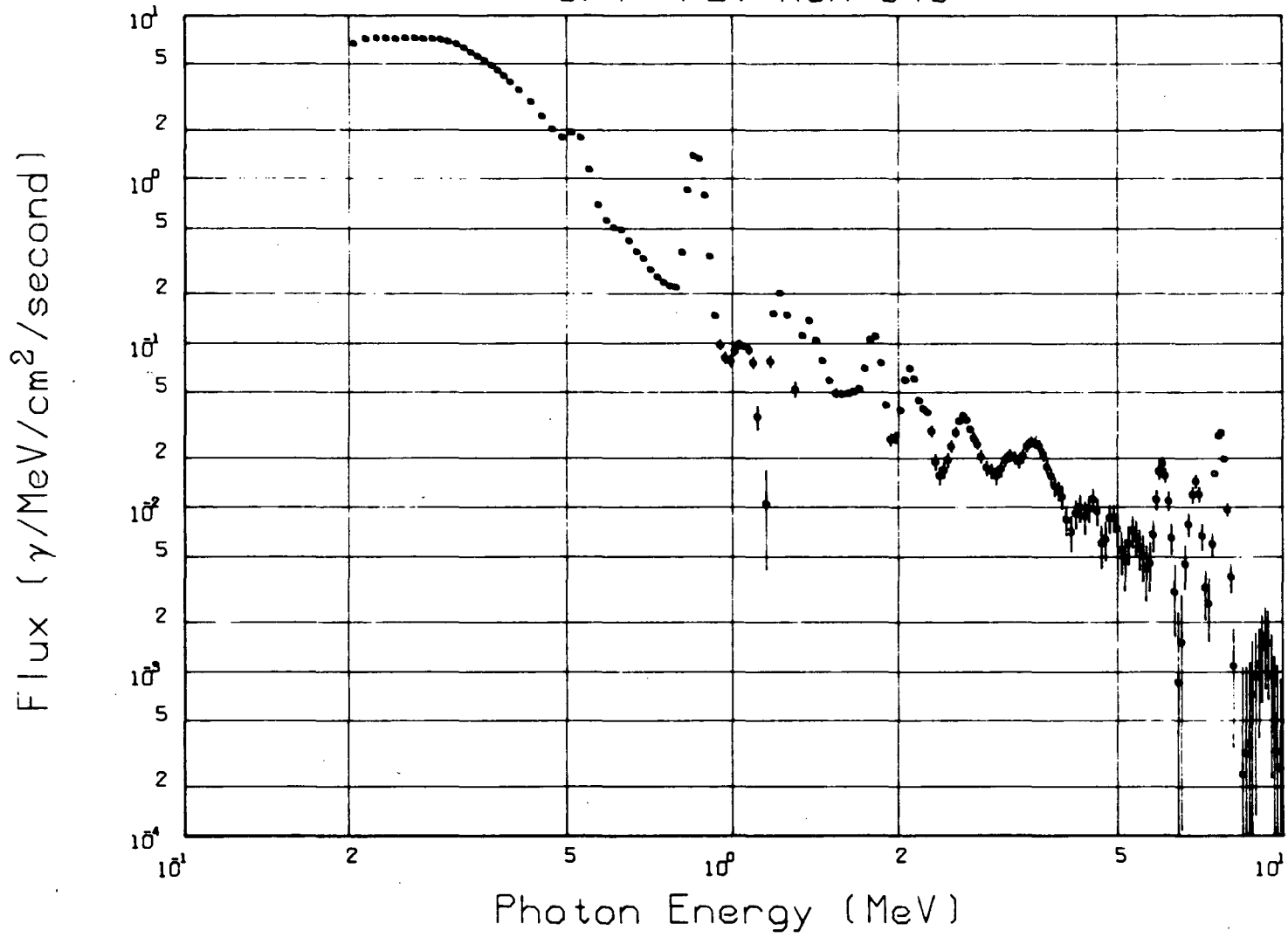


Fig. 10. Gamma Ray Spectra for 1.905-cm-thick Fe Sample

1' FE, RUN 849

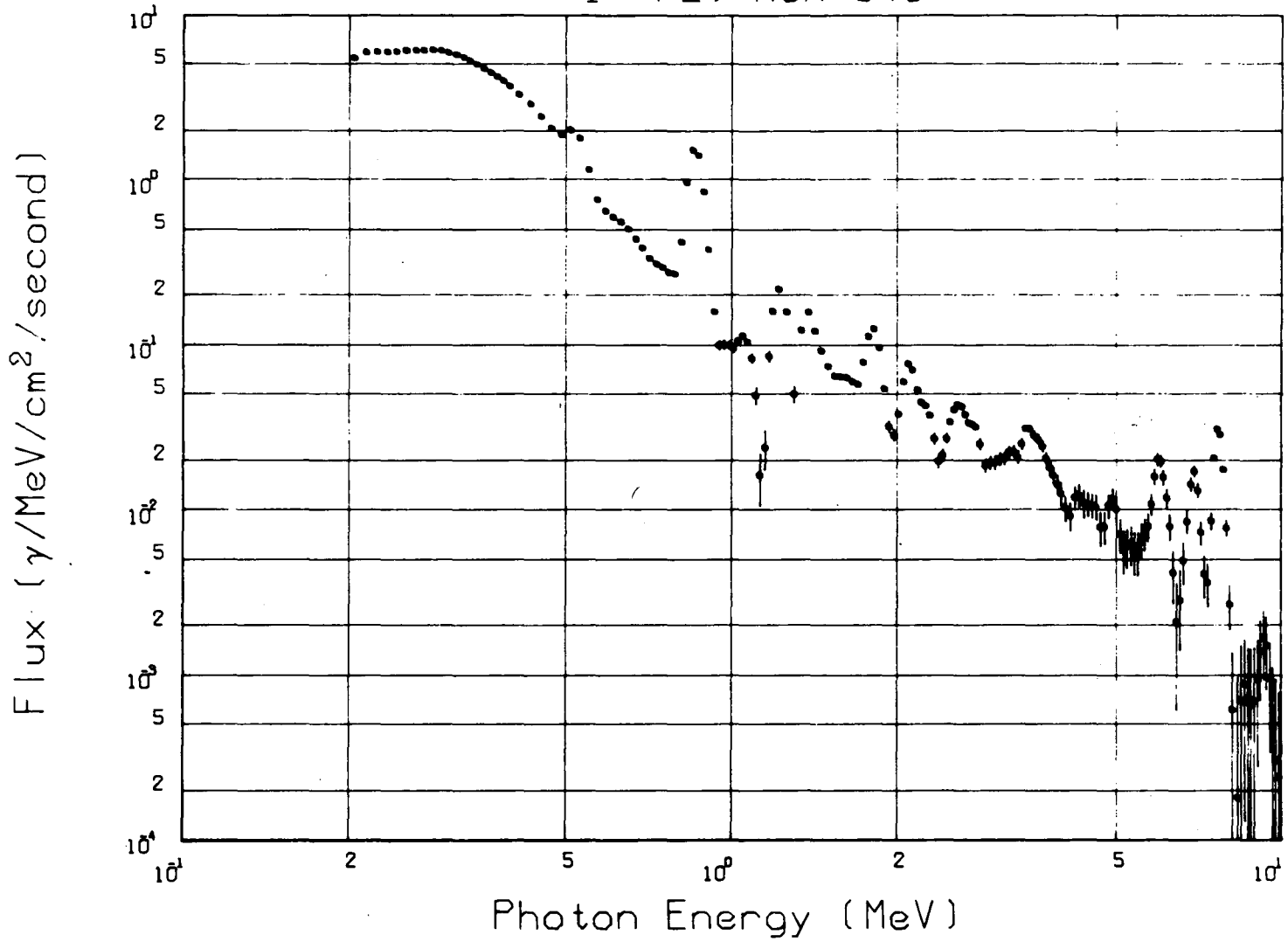


Fig. 11. Gamma Ray Spectra for 2.54-cm-thick Fe Sample

radioactivity. In the first run the thorium sample and Cf^{252} source were used. In the second run the Cf^{252} source was used without the thorium sample but with a plastic bag of equivalent thickness to that containing the thorium in order to account for any gamma rays generated in the plastic. Since the thorium is a radioactive material and hence maintains a high gamma background, a third run was necessary with the sample and no source. Its natural radioactivity makes it difficult to distinguish its peaks from those related to the neutron interaction in the sample. Nevertheless, a peak at 0.186 MeV has been distinguished in the case of thorium as shown in Fig. 12. The unscrambling of the Th^{232} spectrum is shown in Table 7. The fourth run was without source or sample.

RUN 856.7 - 232TH SAMPLE+252CF SOURCE

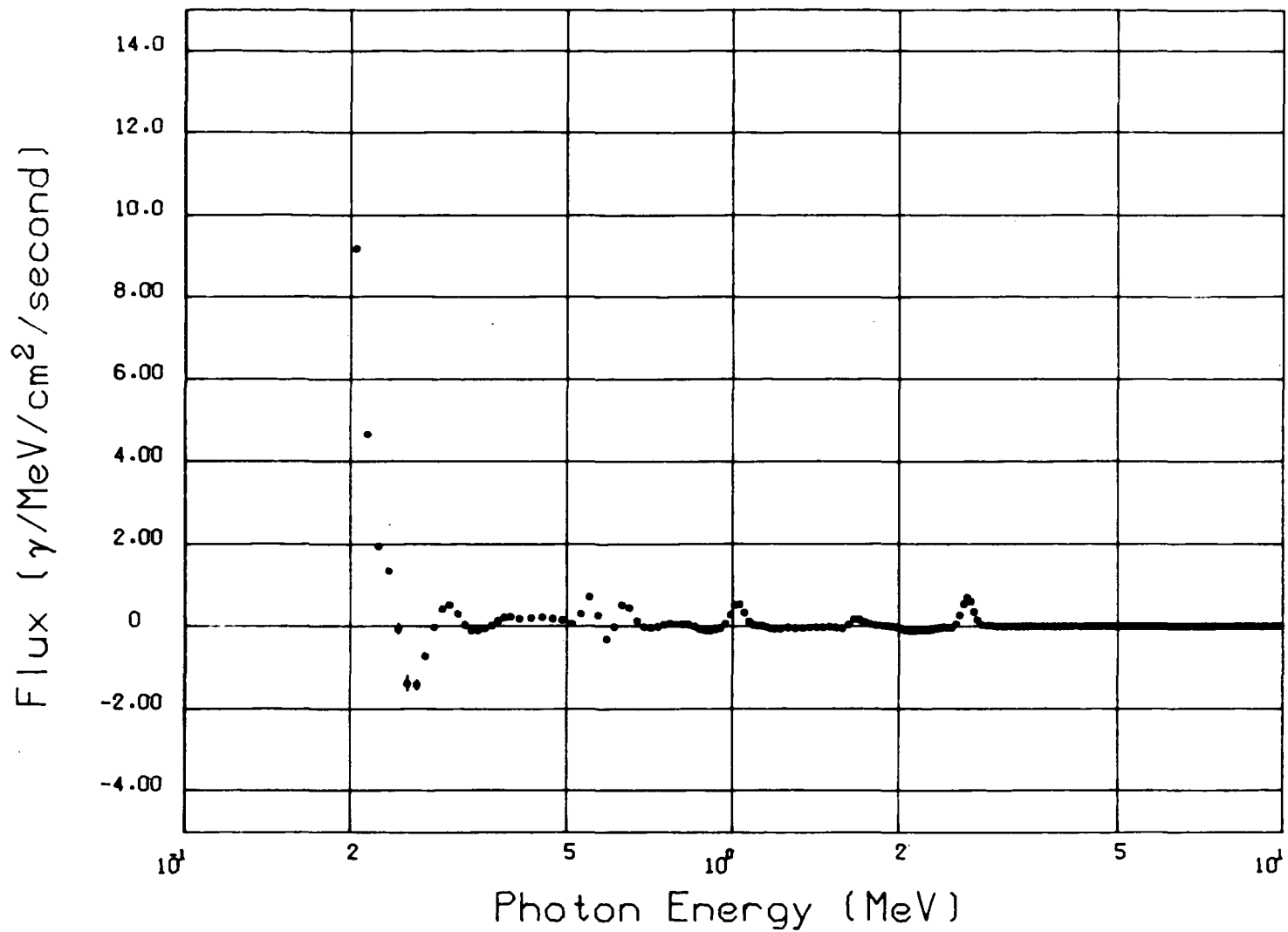


Fig. 12. Gamma Ray Spectra for 1.27-cm-thick Th²³² Sample

Table 7 Gamma Ray Spectral Data for 1.27 cm Th²³² Sample

RUN 856,7 - 232TH SAMPLE+252CF SOURCE

E1 (MEV)	E2 (MEV)	INTEGRAL (G/SQCM/SEC.)	ERROR (G/SQCM/SEC.)
0.205	0.300	8.8677E-02	6.0603E-03
0.300	0.400	1.1784E-02	1.7760E-03
0.400	0.500	1.8608E-02	1.6741E-03
0.500	0.600	2.1900E-02	2.8393E-03
0.600	0.700	2.1958E-02	2.2449E-03
0.700	0.800	1.8449E-03	2.3622E-03
0.800	0.900	-1.0185E-03	2.9578E-03
0.900	1.000	2.9579E-03	2.8328E-03
1.000	1.100	3.0514E-02	9.7777E-04
1.100	1.200	-2.3376E-03	3.4268E-03
1.200	1.300	-4.4843E-03	3.7221E-03
1.300	1.400	-4.4182E-03	3.4475E-03
1.400	1.500	-2.8139E-03	5.3946E-04
1.500	1.600	-3.9578E-03	1.1849E-03
1.600	1.800	2.0689E-02	1.1547E-03
1.800	2.000	1.4592E-03	8.5434E-04
2.000	2.200	-1.9387E-02	1.2433E-03
2.200	2.400	-1.4889E-02	9.8806E-04
2.400	2.600	9.6675E-03	1.6307E-03
2.600	2.800	9.3224E-02	1.6298E-03
2.800	3.000	4.1240E-03	2.4943E-04
3.000	3.500	2.3942E-03	5.3781E-04
3.500	4.000	1.2195E-03	4.9468E-04
4.000	4.500	8.4008E-04	4.6631E-04
4.500	5.000	3.6723E-04	3.9978E-04
5.000	6.000	6.6331E-04	7.0291E-04
6.000	7.000	6.4079E-04	7.5262E-04
7.000	8.000	2.6375E-04	6.1574E-04
8.000	9.000	-2.8440E-04	8.2578E-04
9.000	10.000	-4.1438E-04	1.1029E-03

Calculation was made of the number of photons/cm²/sec for the inelastic scattering peak for Fe (0.846 MeV) to compare it with the area under the same peak obtained by the unscrabbling of the measured spectra.

- A. Calculation of the average cross section ($\bar{\sigma}$) for the 0.846 MeV inelastic gamma ray production in iron using a californium fission neutron spectrum:

<u>E(MeV)</u>	<u>$\Delta\phi(E)$</u>	<u>$\sigma(E)^*$</u>	<u>$\Delta\phi(E).\sigma(E)$</u>
0.8 - 1.0	0.0623595	0.0173	0.0010788
1.0 - 1.5	0.1473782	0.0398	0.0058656
1.5 - 2.0	0.1329588	0.0517	0.0082035
2.0 - 2.5	0.1151	0.08435	0.0097941
2.5 - 3.0	0.0936329	0.090344	0.0084591
3.0 - 4.0	0.1142322	0.100355	0.0114637
4.0 - 5.0	0.0617977	0.107563	0.0066472
5.0 - 6.0	0.0299625	0.11928	0.0035739
6.0 - 7.0	0.0168539	0.12291	0.0020715
7.0 - 8.0	0.0074905	0.125845	0.0009425
8.0 - 9.0	0.0037453	0.12119	0.0004538
9.0 -10.0	0.0018725	0.117335	0.0002197
10.0 -11.0	0.0018725	0.11517	0.0002156
11.0 -12.0	Zero	0.11846	Zero
			Σ 0.0589891

$$\bar{\sigma} = \frac{\int \Delta \phi \{(\sigma(E))\} dE}{\int \Delta \phi (E) dE}$$

considering $\int_{.846}^{12 \text{ MeV}} \phi(E) dE = 1$ (since only those neutrons above .846 MeV can generate inelastic gamma ray)

$$\text{Therefore: } \bar{\sigma} = \frac{0.0589891}{1} = 0.0589 \text{ barns/steradian}$$

Where $\Delta\phi(E)$ is the fraction of neutrons with energy (E) for the californium fission neutron spectrum⁽³⁾, $\bar{\sigma}(E)$ is the cross section for the 0.846 MeV inelastic peak at energy E (differential cross section for the incident neutrons of energy E⁽⁴⁾).

* Barns per steradian.

B. The average attenuation factor of the Fe slabs for the 0.846 MeV inelastic gamma ray peak was obtained by dividing the slab into equal thickness intervals, calculating the attenuation from the center of each interval.

For example, using this technique the 1.27 cm thick Fe slab was divided into 5 regions of .254 cm thickness each.

(1) For the first region the attenuation factor T_1 for

$t = .127$ cm becomes

$$T_1 = e^{-\mu t} = e^{-\frac{.127}{.707}} \times 7.84 \times .0648$$

$$= .91278$$

where $t = \frac{.127}{.707}$ = average Fe thickness for gamma ray to travel

μ = mass attenuation coefficient X density

(2) For the second region $t = \frac{.381}{.707}$ and

$$T_2 = e^{-\mu t} = \frac{.381}{.707} \times 7.84 \times .0648 = .76050$$

Using this procedure the average attenuation factor for all five regions is .65494.

In sequence, then, for all four samples of Fe used in this experiment the average attenuation factors are:

.635 cm Fe - .8039
 1.27 cm Fe - .6549
 1.905 cm Fe - .5469
 2.54 cm Fe - .4628

The attenuation of the 0.846 MeV inelastic gamma ray peak due to 5.64-cm-thick LiH filter in front of the detector collimator and for 237.5 cm of air from sample to detector were calculated to be 0.753 and 0.98 respectively using the same procedure.

The number of neutrons reaching the center of the Fe sample was calculated by

$$n_c = \frac{N_0}{4\pi R_1^2} \quad \text{where, } N_0 = \text{the source}$$

strength at the time of the measurement.

R_1 = the distance from center of source to center of sample.

$$n_c = \frac{2.6 \times 10^8}{12.56 \times (117.9)^2} = 1.489 \times 10^3 \text{ n/cm}^2/\text{sec}$$

Let N_L = the count rate at position L on the sample using 4" Bonner ball.

A_L = the area associated with position L.

T = total neutron/sec reaching the Fe sample.

N_c = count rate at center of sample (4.0×10^4 c/m).

$$\begin{aligned} T &= \sum_{L=1}^L \frac{N_L}{N_c} n_c A_L \\ &= \frac{A_L}{N_c} N_c \sum_{L=1}^{36} N_L \end{aligned}$$

where L = an individual area $10.16 \text{ cm} \times 7.62 \text{ cm} = 77.42 \text{ cm}^2$

$$\sum_{L=1}^{36} N_L = 49.35 \times 10^4 \text{ c/m}$$

$$T = \frac{77.42 \times 1.489 \times 10^3}{4.0 \times 10^4} \times 49.35 \times 10^4 = 1.42 \times 10^6 \text{ n/sec}$$

The number of photons at the detector can be calculated by

$$\phi_\gamma = PT/R_2^2 \text{ (photons/cm}^2/\text{sec)}$$

where P = the probability per steradian per slab thickness @ 45° of a photon being generated

T = n/sec reaching the sample

R_2 = distance from sample to detector
= 237.5 cm

$$P = \text{slab thickness (gm/cm}^2) \times \sigma \text{ (cm}^2\text{/atom)} \\ \times \text{atoms/mol} \div \text{Mol wt sample (g/mol)}$$

For the 1.27 cm sample thickness

$$P = \frac{1.27 \times 7.84}{.707} \times \frac{.0589 \times 10^{-24} \times 6.02 \times 10^{23}}{56} \\ = .008917$$

$$\text{Then } \phi_{\gamma} = \frac{.008917 \times 1.42 \times 10^6}{(237.5)^2} = 0.2245 \text{ photons/cm}^2\text{/sec}$$

Applying a correction to ϕ_{γ} for the attenuation in the Fe sample, LiH, and air,

$$\phi_{\gamma} = 0.2245 \times .6549 \times .753 \times .98 \text{ photons/cm}^2\text{/sec}$$

$$\phi_{\gamma} = .109 \text{ photons/cm}^2\text{/sec}$$

The gamma ray spectra shown in Fig. 9 gives a value of .0747 photons/cm²/sec for the 0.846 MeV gamma ray peak. Using this procedure for all four thicknesses of iron the results from the calculations and measurements can be listed as follows:

<u>Sample Thickness</u>	ϕ_{γ} (photons/cm ² /sec)	
	<u>Calculation</u>	<u>Measurement</u>
.635 cm Fe	0.0667	0.0422
1.27 cm Fe	0.109	0.0747
1.905 cm Fe	0.136	0.0899
2.54 cm Fe	0.154	0.984

This is about 30% lower than the calculated value. There is some reason to believe that the Fe cross section is not correct. Neutron attenuation in the iron has not been taken into account here, but the feeling is that elastic scattering in the iron tends to compensate for any attenuation, particularly with samples of this thickness. The agreement between measurement and calculation for four different thicknesses

used here tends to corroborate the assumption. There is also a background of scattered neutrons from the collimator which are not included in this calculation. This background will be accurately evaluated at a later date; however, existing measurements indicate that the magnitude of this background is about 10%. This would increase the calculated value for the 0.846 gamma ray by roughly this amount, depending in detail on the spectrum of the background neutrons. Very recent results⁽⁶⁾ obtained after this work was completed indicate that the 0.846 MeV inelastic gamma ray yield from iron is anisotropic so that these calculated results should be multiplied by a factor of 0.81.

The Th²³² slab used in the measurements was in the form of a circular disc 30 cm in diameter and 1.27 cm thick enclosed in a plastic bag 24 mils thick for safe handling. Four different measurements were required to obtain gamma spectra from neutrons interacting with the thorium. In the first measurement the background of the sample was taken without the source as Th²³² is a radioactive material. The second measurement was taken for the source on and the Th²³² slab at 45° to the intersection of the axis of the detector collimator axis with the neutron beam centerline. The third measurement included the source and an equivalent thickness of plastic to that surrounding the sample. The fourth measurement was of the background of the detector shield with source or sample so that it could be added to the foreground to compensate for a double subtraction in the previous two measurements for the background. The unscrambled spectrum for Th²³² is shown in Fig. 12. As the unfolding method did not go below 0.2 MeV the inelastic peak for Th²³² or 0.186 MeV is not totally unscrambled. It can, however, be estimated from the analyzer spectrum. The high intensity gamma radiation background from the natural Th²³² sample itself makes it difficult to distinguish other possible peaks due to interaction of neutrons from the californium source with the Th²³² sample.

To our knowledge a measurement or calculation of the integral or differential cross sections for gamma ray production in thorium from inelastically scattered neutrons does not exist. Thus, the purpose of this measurement was an attempt to generate an integral cross section using a Cf²⁵² source.

Theoretical calculations as derived by E. M. Oblow⁽⁵⁾, can be reduced to a simple expression for determining such a cross section.

$$\Sigma_{n\gamma} = \frac{\mu k_{\gamma}}{.707 k_n}$$

where $\Sigma_{n\gamma}$ = the integral cross section for the production of gamma rays from inelastically scattered californium neutrons.

μ = attenuation coefficient for gamma rays in thorium (17.05 cm⁻¹).

k_{γ} = number of gamma rays/sec produced in the sample.

k_n = number of neutrons/sec incident on the sample.

The value .707 is inserted into the expression to convert the current to flux.

The values of k_{γ} and k_n can be calculated as follows:

$$k_{\gamma} = \frac{\text{counts}}{\text{sec}} \cdot \frac{1}{e} \cdot \frac{4 R_2^2}{R_3^2}$$

where counts/sec = number of counts in gamma ray peak = 46.4

e = efficiency of NaI crystal = ~ 1 .

R_3 = radius of NaI crystal = 6.35 cm.

R_2 = distance from sample to detector = 237.5 cm.

k_{γ} = 2.60×10^5 gamma/sec.

k_{γ} must be corrected for attenuation in LiH (1.85) and air (1.035).

Therefore: $k_{\gamma} = 2.60 \times 10^5 \times 1.85 \times 1.035 = 4.98 \times 10^5$ gamma/sec
 $\mu = 17.05 \text{ cm}^{-1}$

Using the same method as described previously for the iron sample, number of the neutrons incident on the sample becomes

$$k_n = \frac{77.42 \times 1.489 \times 10^3}{4 \times 10^4} \times 30.92 \times 10^4 = 8.91 \times 10^5 \text{ n/sec}$$

$$\text{Then } \Sigma_{n\gamma} = \frac{17.05 \times 4.98 \times 10^5}{.707 \times 8.91 \times 10^5} = 13.5 \text{ cm}^{-1}$$

This cross section value, when converted to barns, is considerably higher than should be expected when compared to the total cross section. Further measurements will be made at a later date to determine if this discrepancy was due to an error in the experimental procedure or if some phenomena other than neutron interaction with the sample is responsible.

List of Tables

	<u>Page No.</u>
Table 1 Vertical Mapping of Detector Collimator.....	9
Table 2 Horizontal Mapping of Detector Collimator.....	10
Table 3 Gamma Ray Spectral Data for .635 cm Fe	13
Table 4 Gamma Ray Spectral Data for 1.27 cm Fe.....	14
Table 5 Gamma Ray Spectral Data for 1.905 cm Fe.....	15
Table 6 Gamma Ray Spectral Data for 2.54 cm Fe.....	16
Table 7 Gamma Ray Spectral Data for 1.27 cm Th ²³² Sample...	23

List of Figures

	<u>Page No.</u>
Fig. 1. Sketch of the Experimental Layout in Scale.....	2
Fig. 2. Sketch Showing the Source Collimator Only.....	3
Fig. 3. Count Rate Against Horizontal Distance of the Bonner Ball Along the Source Collimator (6 runs).....	4
Fig. 4. A Contour Map of the Neutron Intensities Obtained From the Six Mapping Runs.....	5
Fig. 5. Vertical Mapping of the Detector Collimator Using a Co ⁶⁰ Gamma Source.....	7
Fig. 6. Horizontal Mapping of the Detector Collimator Using a Co ⁶⁰ Gamma Source.....	8
Fig. 7. Response Functions for the NaI (Tl) Crystal.....	12
Fig. 8. Gamma Ray Spectra for .635-cm-thick Fe Sample.....	17
Fig. 9. Gamma Ray Spectra for 1.27-cm-thick Fe Sample.....	18
Fig. 10. Gamma Ray Spectra for 1.905-cm-thick Fe Sample.....	19
Fig. 11. Gamma Ray Spectra for 2.54-cm-thick Fe Sample.....	20
Fig. 12. Gamma Ray Spectra for 1.27-cm-thick Th ²³² Sample.....	22

REFERENCES

1. R. E. Maerker, F. J. Muckenthaler, "Gamma Ray Spectra Arising from Fast Neutron Interactions in Elements Found in Soils, Concretes and Structural Materials," ORNL-4475 (1970).
2. W. R. Burrus, "Utilization of Apriori Information in the Statistical Interpretation of Measured Distributions," Dissertation, The Ohio State University, ORNL-3743 (1964).
3. R. M. Freestone, Jr., " Cf^{252} Fission Neutron Spectrum," Private communication (1976).
4. G. T. Chapman, A Remeasurement of the Neutron Induced Gamma Ray Production Cross Sections for Iron in the Energy Range $850 \text{ keV} \leq E_n \leq 20 \text{ MeV}$," ORNL/TM-5416 (July 1976).
5. E. M. Oblow, Private Communication, (1976).
6. W. E. Kinney, F. G. Perey, "High Resolution Fast Neutron Gamma Ray Production Cross Sections for Iron up to 2100 keV." (NSE article to be published.)

1

10/10/10

Dear Sir,
I have the pleasure to inform you that your application for the position of [Job Title] has been successful. We are pleased to have you join our team.

Your starting date will be [Date]. We will be in contact with you regarding the details of your employment, including your salary and benefits package.

Please contact [Name] at [Phone Number] or [Email Address] if you have any questions. We look forward to meeting you and welcoming you to the company.

Yours faithfully,
[Name]
[Title]

Internal Distribution

- | | | | |
|------|--------------------|--------|---|
| 1-3. | L. S. Abbott | 9. | F. R. Mynatt |
| 4. | C. E. Clifford | 10-11. | Central Research Library |
| 5. | K. M. Henry | 12. | ORNL Y-12 Technical Library
Document Reference Section |
| 6. | R. E. Maerker | 13-14. | Laboratory Records |
| 7. | F. C. Maienschein | 15. | Laboratory Records ORNL RC |
| 8. | F. J. Muckenthaler | 16. | ORNL Patent Office |

External Distribution

- 17-20. Argonne National Laboratory (ERDA)
- 21-23. Battelle - Northwest (ERDA)
- 24-25. Bettis Atomic Power Laboratory (ERDA)
- 26-29. Brookhaven National Laboratory (ERDA)
- 30. ERDA Chicago Operations Office
- 31. ERDA Division of Physical Research
- 32. ERDA Division of RRD, Physics Branch
- 33-34. Los Alamos Scientific Laboratory (ERDA)
- 35. Mound Laboratory (ERDA)
- 36-62. Technical Information Center (TIC)
- 63. Dr. I. Hamruda, Director of Nuclear Research Center,
Cairo, Egypt
- 64. Dr. A. Elkadi, Head of the Reactor and Neutron Physics
Division, Atomic Energy Establishment, Cairo, Egypt
- 65-70. A. S. Makarious, Reactor and Neutron Physics Division,
Atomic Energy Establishment, Cairo, Egypt
- 71. Director, Research and Technical Support Division, ERDA-ORO